Author Manuscript

Author Manuscript

Author Manuscript

Author Manuscript

HHS Public Access

Author manuscript

Prog Retin Eye Res. Author manuscript; available in PMC 2018 March 01.

Published in final edited form as:

Prog Retin Eye Res. 2017 March ; 57: 76–88. doi:10.1016/j.preteyeres.2016.11.001.

Adaptive Optics Optical Coherence Tomography in Glaucoma

Zachary M. Dong[1], **Gadi Wollstein**[2], **Bo Wang**[1], and **Joel S. Schuman**[2,3]

[1]University of Pittsburgh Medical Center (UPMC) Eye Center, Eye and Ear Institute, Department of Ophthalmology, University of Pittsburgh School of Medicine, Ophthalmology and Visual Science Research Center, Pittsburgh, Pennsylvania, United States

[2]New York University (NYU) Langone Eye Center, NYU Langone Medical Center, Department of Ophthalmology, NYU School of Medicine, New York, New York, United States

[3]Department of Electrical and Computer Engineering, New York University Tandon School of Engineering, Brooklyn, New York, United States

Abstract

Since the introduction of commercial optical coherence tomography (OCT) systems, the ophthalmic imaging modality has rapidly expanded and it has since changed the paradigm of visualization of the retina and revolutionized the management and diagnosis of neuro-retinal diseases, including glaucoma. OCT remains a dynamic and evolving imaging modality, growing from time-domain OCT to the improved spectral-domain OCT, adapting novel image analysis and processing methods, and onto the newer swept-source OCT and the implementation of adaptive optics (AO) into OCT. The incorporation of AO into ophthalmic imaging modalities has enhanced OCT by improving image resolution and quality, particularly in the posterior segment of the eye. Although OCT previously captured *in-vivo* cross-sectional images with unparalleled high resolution in the axial direction, monochromatic aberrations of the eye limit transverse or lateral resolution to about 15-20 μm and reduce overall image quality. In pairing AO technology with OCT, it is now possible to obtain diffraction-limited resolution images of the optic nerve head and retina in three-dimensions, increasing resolution down to a theoretical 3 μm^3. It is now possible to visualize discrete structures within the posterior eye, such as photoreceptors, retinal nerve fiber layer bundles, the lamina cribrosa, and other structures relevant to glaucoma. Despite its limitations and barriers to widespread commercialization, the expanding role of AO in OCT is propelling this technology into clinical trials and onto becoming an invaluable modality in the clinician's arsenal.

Corresponding Author Joel S. Schuman, MD, NYU Langone Medical Center, Department of Ophthalmology, New York University School of Medicine, 462 First Avenue, NBV 5N3, New York, New York. 10016. United States of America. Joel.Schuman@nyumc.org.
dongzm@upmc.edu; gadi.wollstein@nyumc.org; wangb4@upmc.edu; joel.schuman@nyu.edu

Publisher's Disclaimer: This is a PDF file of an unedited manuscript that has been accepted for publication. As a service to our customers we are providing this early version of the manuscript. The manuscript will undergo copyediting, typesetting, and review of the resulting proof before it is published in its final citable form. Please note that during the production process errors may be discovered which could affect the content, and all legal disclaimers that apply to the journal pertain.

Disclosure: Z.M. Dong, None; G. Wollstein, None; J.S. Schuman, Zeiss (C, P), Aerie (C), Annexon (C), Alcon (C), Opticient (C), Shire (C), Pfizer (C), SLACK/Vindico (C)

Author Manuscript Author Manuscript Author Manuscript Author Manuscript

1. Background

Glaucoma is a slowly progressive, multifactorial, degenerative optic neuropathy and is the most common cause of irreversible blindness and the second most common cause of blindness worldwide (Quigley and Broman, 2006). Glaucoma is characterized by the degeneration of retinal ganglion cells (RGCs) and their axons, associated with morphological changes within the optic nerve and retinal nerve fiber layer (RNFL) (Garcia-Valenzuela et al., 1995; Quigley, 2011; Quigley et al., 1989; Quigley et al., 1995; Sommer et al., 1977; Weinreb et al., 2014; Weinreb and Khaw, 2004) such as neuroretinal rim thinning and RNFL wedge defects. Accurate and early detection of glaucomatous structural changes is paramount to successful management and the prevention of disease progression considering that the disease is causing irreversible loss of visual function (Foster et al., 2002; Quigley and Broman, 2006).

1.1 Optical coherence tomography

Optical coherence tomography (OCT) is one modality that has become particularly widespread and is now the state-of-the-art imaging modality in glaucoma, supplanting older adjuncts for glaucoma diagnosis and monitoring (Girach and Sergott, 2016). OCT was first demonstrated in 1991 (Huang et al., 1991) as an application of low-coherence interferometry (Fercher et al., 1988). In 1993, the first OCT imaging studies of the human retina *in-vivo* were performed; and the devices became commercially available in 1996 after scanning patterns with reproducible measurements were developed (Schuman et al., 1996). The groundbreaking technique has allowed for *in-vivo*, noninvasive, high-resolution cross-sectional imaging of ocular structures. With the ability to provide quantitative evaluation of neural structures affected by the disease, such as the macula, RNFL, and optic nerve head (ONH) (Kim et al., 2010; Leite et al., 2011; Leung et al., 2009; Leung et al., 2010; Medeiros et al., 2004; Park et al., 2009; Rao et al., 2010; Sehi et al., 2009; Wang et al., 2011b), its clinical utility was quickly realized (Puliafito et al., 1995; Schuman et al., 1995). OCT began to gain popularity in clinical ophthalmology in the early 2000's. OCT has since changed the paradigm of visualization of the retina and revolutionized the management and diagnosis of glaucoma, being widely used for the initial assessment of glaucoma and for monitoring disease progression and response to its various treatment modalities (Mansouri et al., 2013b; Puliafito, 2010).

1.1.2 Advances in optical coherence tomography—Since its initial introduction, OCT technology has advanced considerably. Previously available OCT instruments used a technique referred to as time-domain (TD-) OCT. TD-OCT was based on the low coherence interferometry principle of signal reflected from the eye and signal from an oscillating reference mirror, in order to match path lengths with separate reflective surfaces within the retina. The first commercially available TD-OCT (Stratus OCT, Zeiss, Dublin, CA), featured nominal axial resolution of 10 μm, transverse resolution of 20 μm, and scanning speed of 400 axial scans per second. However, this technology was limited by suboptimal resolution and slow scan acquisition rates (Hougaard et al., 2007a, b; Lee et al., 2009; Manassakorn et al., 2006; Medeiros et al., 2009b; Medeiros et al., 2005; Naithani et al., 2007; Nouri-

Author Manuscript Author Manuscript Author Manuscript Author Manuscript

Mahdavi et al., 2008; Parikh et al., 2007; Wollstein et al., 2005). Hardware advances in commercial systems improved resolution and increased scanning speeds.

The introduction of spectral-domain (SD-) OCT increased scan acquisition rate, allowing for a more thorough sampling of the area of interest and greatly reduced the need for interpolation between adjacent scans as compared to TD-OCT (Gonzalez-Garcia et al., 2009; Iliev et al., 2006; Kim et al., 2009; Knight et al., 2009; Leitgeb et al., 2003; Leung et al., 2009; Leung et al., 2011; Mwanza et al., 2011; Ortega Jde et al., 2009; Schuman, 2008; Sung et al., 2011). In this iteration of the technology, the reference arm is stationary and interference pattern from the sampling and reference arms are detected spectroscopically. Image analysis of neuro-retinal features has also advanced significantly since the introduction of OCT in the clinic. Initially, RNFL was the only feature of the retina measured by OCT that was used for glaucoma management, providing objective, quantitative measurements of RNFL thickness (Huang et al., 1991). However, when newer SD-OCT devices began to measure and quantify additional structural features, such as those from the ONH and macula, the clinical utility increased for OCT in glaucoma.

Since its commercialization, SD-OCT has become available from numerous manufacturers and has been established as the dominant imaging modality in the management of glaucoma. The nominal axial resolution of the commercial devices range between 3 to 7 μm, transverse resolution is similar across devices at 20 μm, but the scanning speed varies between 25,000 to 100,000 axial scans per seconds. Scan patterns and measurements across these devices are generally not interchangeable, but their ability to detect glaucomatous changes of the fundus are similar (Akashi et al., 2013; Leite et al., 2011; Pierro et al., 2012). Overall, SD-OCT devices enhanced reproducibility and accuracy in quantifying glaucomatous damage.

Swept-source OCT (SS-OCT), a newer generation of OCT, has recently been introduced (Chinn et al., 1997). SS-OCT utilizes a longer wavelength (generally 1050 nm) compared with SD-OCT (840 nm). SS-OCT systems are able to capture high resolution images of the anterior chamber (AC) improving visualization and quantification of the AC structures. Because SS-OCT devices are less susceptible to signal attenuation, compared with other iterations of the technology, they are helpful in evaluating deeper posterior segment ocular structures, such as the choroid and lamina cribrosa (LC) *in-vivo* (Mansouri et al., 2013a; Mansouri et al., 2013b; Park et al., 2014; Takayama et al., 2013). SS-OCT has enabled users to acquire high quality wide-angle scans that contain a large area of the posterior pole, including both the optic disc and macula.

1.2 Adaptive optics for ophthalmic imaging

The addition of adaptive optics (AO) into ophthalmic imaging modalities has further enhanced image quality. Before AO was introduced into ocular imaging with retinal cameras (Liang et al., 1997), the technique was already highly utilized in astronomy imaging protocols to reduce atmospheric distortion caused by diffraction. Specifically, AO has helped reduce speckle or granular image artifacts, minimize blur, and resolve faint features of astrophysical objects when viewing from ground-based telescopes. To accomplish this, AO systems employ a wavefront sensor and wavefront corrector to measure and correct optical

Author Manuscript Author Manuscript Author Manuscript Author Manuscript

aberrations in real time, typically with a deformable mirror that compensates for the aberrations by changing the shape of the incoming wavefront (Lombardo et al., 2013).

AO technology seeks to correct for the eye's optical aberrations and has been adapted to multiple ophthalmic imaging modalities (Godara et al., 2010; Williams, 2011). These optical aberrations impose a limit on ophthalmic imaging devices, resulting in blurring and image artifacts (Charman and Chateau, 2003; Guirao et al., 2002; Thibos et al., 2002b).

Although defocus, such as myopia and hyperopia, and astigmatism account for majority of optical aberrations in human eyes, “high-order” wavefront aberrations exist even in normal eyes (Castejon-Mochon et al., 2002; Porter et al., 2001; Williams et al., 2000). The development of wavefront sensors in the 1990's has allowed for researchers to routinely measure these aberrations (Castejon-Mochon et al., 2002; Diaz-Santana et al., 2003; Guirao et al., 2002; Lombardo and Lombardo, 2009; Lombardo et al., 2013; Nirmaier et al., 2003; Porter et al., 2001; Salmon and van de Pol, 2006; Thibos, 2000; Thibos et al., 2002a; Wang et al., 2003b). AO corrects for these aberrations and theoretically can improve image quality from any ophthalmic instrument involving the passing of light into or out of the eye. Adapting AO technology from concept to ocular imaging modalities, however, requires substantial engineering efforts.

1.2.1 Adaptive optics and optical coherence tomography—Since its introduction into ophthalmic imaging in 1989 (Dreher et al., 1989), AO technology has been successfully integrated into multiple ocular imaging modalities, including conventional fundus cameras (Bedggood and Metha, 2012; Dees et al., 2011; Liang et al., 1997; Rha et al., 2006; Salas et al., 2016), scanning laser ophthalmoscopy (SLO),(Burns et al., 2007; Dreher et al., 1989; Dubra and Sulai, 2011; Roorda et al., 2002) OCT (Torti et al., 2009; Wang et al., 2011a; Zawadzki et al., 2009; Zhang et al., 2005), or some combination of these (Hammer et al., 2012; Salas et al., 2016). In 1997, AO was first integrated into fundus cameras (Liang et al., 1997). The first AO-SLO was successfully demonstrated in 2002 (Roorda et al., 2002), showing the confocal advantages of SLO in the measurement of rudimentary optical sectioning and blood cell velocity. This was closely followed by the pairing of AO with OCT devices (Fernandez et al., 2005; Zawadzki et al., 2005; Zhang et al., 2005) with expanded applications in the founding labs (Miller et al., 1996; Merino et al., 2006; Jonnal et al., 2010; Kurokawa et al., 2010; Jonnal et al., 2016; Salas et al., 2016). Soon, many targeted improvements in AO-OCT system design and performance were reported by an increasing number of laboratories researching AO-OCT (Cense et al., 2009a; Diaz-Santana et al., 2003; Fernandez et al., 2008; Kocaoglu et al., 2011a; Kurokawa et al., 2010; Merino et al., 2006; Torti et al., 2009; Zawadzki et al., 2009; Zawadzki et al., 2007).

OCT and AO have fundamentally improved ONH and retinal imaging and are complementary technologies allowing for resolution at a microscopic level. Although SD-OCT is already a proven and well-established imaging modality that captures *in-vivo* cross-sectional images with unparalleled high resolution in the axial direction, monochromatic aberrations of the eye limit lateral resolution to about 15-20 μm and reduce overall image quality. Since AO helps correct for these aberrations, imaging obtained with AO-OCT has substantially improved lateral resolution (Hermann et al., 2004; Hofer et al., 2001; Porter et

Author Manuscript Author Manuscript Author Manuscript Author Manuscript

al., 2001). This is a major advantage of AO-OCT systems as its axial resolution of 3–8 μm is substantially better when compared to other systems. AO-OCT corrects for the eye's optical aberrations most commonly with a Shack-Hartmann configuration (Liang et al., 1994; Platt and Shack, 2001) with wavefront sensors and electro-actuated deformable mirrors.

Similar to the benefits seen in astronomy, AO also reduces the high-contrast granular image artifacts that obscure microscopic details, which are characteristically inherent to OCT due to its interferometric nature. Speckle size of AO-OCT systems have been observed to be as much as 9.6 times smaller than that of conventional SD-OCT when AO is paired with ultra-high resolution OCT (Kocaoglu et al., 2011a). In this case, speckle size was reduced from 7.3 μm (axial) × 11.4 μm (lateral) in SD-OCT (Spectralis, Heidelberg Engineering) to 2.9 μm × 3.0 μm in AO-OCT device. In order to reach AO's full resolving potential, minimize lateral speckle, and obtain the transverse resolution needed to view individual cells, the pupil should ideally be large (greater than 5 mm) (Artal et al., 2001; Fernandez and Drexler, 2005; Donnelly and Roorda, 2003; Liang et al., 1997; Miller et al., 2003; Porter et al., 2006). Furthermore, OCT systems outfitted with AO technology are more sensitive to weak retinal reflectance, capturing a measured improvement of about 4–8 dB (Cense et al., 2009a). In these ways, the two technologies are complementary in obtaining nearly diffraction-limited resolution images of the ONH and retina in three-dimensions (3D), providing a theoretical spot volume of 3 μm^3; and it now possible to visualize discrete structures within the posterior eye, such as individual cells and photoreceptors.

1.2.1.1 Current drawbacks of AO-OCT: AO-OCT has limitations, however, and many of them are obstacles to widespread adoption of this technology into clinical practice. Because AO-OCT can often have a limited field of view, acquiring a series of neighboring scans to compile an image covering a larger volume may be advantageous (Burns et al., 2007), though the extend acquisition time is a major clinical obstacle. Furthermore, because of the limited depth of focus, patching together volumes or adjusting the focal plane may be necessary in order to fully visualize the retinal structures at varying depths (Fernandez et al., 2005; Zawadzki et al., 2009). Nadler et al., in seeking to characterize the LC *in-vivo* with AO-OCT, used the exterior margin of the optic disc for determining the extent of visible LC; however, the authors noticed that the AO-OCT's narrow depth of focus hindered the identification of the scleral canal opening, which is standard feature for delineation of the disc boundary (Nadler et al., 2014a). AO-OCT instruments that can be used for retinal imaging have yet to efficiently integrate strategies to overcome this limitation, such as quickly recording multiple volumes with differing axial focal positions or employing special beams with non-Gaussian intensity distributions.

Apart from these limitations, some of the barriers to more widespread commercialization include the requisite need of expertise and adequately trained personnel and the implementation of robust image processing and analysis tools in friendly graphic user interfaces. More recent technological developments in AO-OCT retinal imaging systems have potential to overcome some of these barriers to integration into clinics. For example, novel SS-OCT systems outfitted with AO have substituted the Hartmann-Shack Wavefront Sensor, which are typically built with concave mirrors, with a wavefront sensorless adaptive optics algorithm paired with lens-based optical systems (Jian et al., 2016). This change

Author Manuscript Author Manuscript Author Manuscript Author Manuscript

maintains diffraction limited imaging while reducing overall system size and complexity. The continual development of more robust, straightforward, and user-friendly AO-OCT devices is needed to assist with increasing access to the technology. And the cost of AO-OCT devices will undoubtedly decrease with increasing demand.

Other barriers include ocular motion artifacts and barriers involved in the processing of images obtained from AO devices. Although high speed AO-OCT systems and retinal tracking techniques are now available and help reduce image artifacts (Ishikawa et al., 2006; Kocaoglu et al., 2014a; Kocaoglu et al., 2014b; Zawadzki et al., 2014), it is still unclear whether these provide better ability to detect disease (Menke et al., 2009). Additionally, novel post-processing methods (Jonnal et al., 2012), and high-speed complementary metal oxide semiconductor (CMOS) detectors have been employed to reduce motion artifacts (Kocaoglu et al., 2011b; Kocaoglu et al., 2011c; Salas et al., 2016). The time required to obtain, process, and analyze images are also hindrances to AO-OCT's transition from lab to clinic; AO-OCT's clinical utility will increase with the development of novel sensitive metrics and image analysis strategies.

Furthermore, normative databases are required to define what constitutes normality. Although, for example, determining capillary density, quantifying blood flow, characterizing LC microstructure, and measuring RNFL bundles, are currently possible with AO technology, reference databases for these assays and disease states are currently lacking and are needed in order to discriminate healthy from glaucomatous eyes. This is especially true as AO uncovers new structures and features, which, just as photoreceptor spacing and density, require validation and need to be described in quantitative terms.

2. The expanding role of AO-OCT

Despite these drawbacks, OCT technology is advancing rapidly and the increasing role of AO is helping to propel AO-OCT into clinical trials and onto becoming an invaluable modality in the clinician's arsenal. Significant cellular damage has often already occurred by the time pathology is visible with current imaging tools - a reality that is now widely appreciated. Considering AO-OCT's abilities, the clinical implications are exciting, such as diagnosing retinal diseases early or more sensitive evaluation of treatment response at the cellular level. Individual RNFL bundles are now able to be visualized *in-vivo*, for example, along with retinal capillaries and other microvasculature (Hammer et al., 2008; Martin and Roorda, 2009; Popovic et al., 2011; Schmoll et al., 2011; Tam et al., 2010; Tam et al., 2011; Wang et al., 2011a; Zhong et al., 2011), Henle's fiber layer, RGCs and other microscopic structures in this layer, photoreceptor mosaic; retinal pigment epithelium, and details of the LC microstructure. In addition to glaucoma, AO technology is valuable for numerous other clinical applications and it is currently being used to study a number of clinical conditions, including macular degeneration, hereditary retinal dystrophies, retinopathy of prematurity, and other optic neuropathies.

2.1 Photoreceptors

Photoreceptors were one of the first targets of studies implementing AO-adapted ophthalmic imaging (Chen et al., 2011; Choi et al., 2006; Cooper et al., 2011; Dubra et al., 2011;

Author Manuscript Author Manuscript Author Manuscript Author Manuscript

Genead et al., 2011; Talcott et al., 2011; Tojo et al., 2013; Wolfing et al., 2006) and some of these findings are relevant to glaucoma. Improvements in AO-SLO performance significantly reduced monochromatic aberrations within AO-SLO systems and, for the first time, enabled a clear visualization of photoreceptors (Dubra and Sulai, 2011; Dubra et al., 2011). Although glaucoma is considered a disease of the inner retina, several studies have shown there may be an effect on the outer retina (Buchi, 1992; Fazio et al., 1986; Holopigian et al., 1990; Kendell et al., 1995; Nork et al., 2000; Odom et al., 1990; Panda and Jonas, 1992; Poinoosawmy et al., 1980; Pokorny and Smith, 1986; Vaegan et al., 1995; Wygnanski et al., 1995). Photoreceptor loss and insult in glaucoma eyes have been observed in histology (Buchi, 1992; Nork et al., 2000), while intraocular pressure (IOP) elevation, was associated with a reduction in photoreceptor responses in rodents (He et al., 2006; Kong et al., 2009; Sun et al., 2007). One recent study of patients with permanent, glaucoma-like visual field (VF) abnormalities in other optic neuropathies, such as optic neuritis, ONH drusen, pseudotumour cerebri, and non-arteritic ischemic optic neuropathy, all revealed structural changes in cones along with expected inner retinal changes (Choi et al., 2008).

More recently, morphological changes in the photoreceptors have been directly assessed *in-vivo* in glaucoma eyes with the aid of AO-OCT (Choi et al., 2011). In that study, which included a wide range of glaucomatous conditions, from pre-perimetric disease to advanced glaucoma with corresponding VF defects, ultra-high resolution AO-OCT revealed outer retinal changes and identified the exact location of structural changes within the cone photoreceptor layer. Concurrent AO-fundus camera images showed corresponding dark areas in the cone mosaic at the same retinal locations with reduced visual sensitivity. In AO-OCT, AO-fundus camera, and AO-SLO, individual healthy photoreceptors appear as bright spots (Figure 1), which is due to the high refractive index relative to the surroundings, strong directional coupling of light by the photoreceptor inner segment into the outer segment (Miller et al., 1996), and backscattering due to mirror-like reflections from each of the outer segment layers (Kocaoglu et al., 2011c). Although the photoreceptor mosaic's precise role in glaucoma is not yet fully elucidated, AO technology provides the means to resolve this issue. Going forward, new models for understanding the complex photoreceptor-light interaction are also important for experiments aimed at improving diagnostic ophthalmic imaging devices (Vohnsen, 2014).

2.2 Retinal nerve fiber layer

Ophthalmic imaging modalities with the ability to detect and track pathological changes of the retinal structures, such as the RNFL, at an early, pre-symptomatic stage of disease represent the basis for developing new diagnostic and management protocols in glaucoma. Currently, diagnosis of glaucoma is confirmed based on the presence of typical VF defects on standard automated perimetry (SAP) and corresponding signs of glaucomatous ONH and retinal damage; and thus the diagnosis of moderate to severe cases of glaucoma is relatively straightforward. However, it is often thought that glaucomatous structural damage precedes vision loss (Artes and Chauhan, 2005; Kuang et al., 2015; Medeiros et al., 2009a; Quigley et al., 1992; Sommer et al., 1991; Strouthidis et al., 2006; Wollstein et al., 2005) with the disease frequently remaining asymptomatic in its early stages. It is worth noting that observed pre-perimetric structural losses could be an artifact of the testing method. SAP

Author Manuscript Author Manuscript Author Manuscript Author Manuscript

only has the ability to detect functional deficits after at least 25–50% of RGCs have undergone apoptosis (Harwerth et al., 1999; Kerrigan-Baumrind et al., 2000; Medeiros et al., 2013; Miglior et al., 2005; Mwanza and Budenz, 2015; Quigley et al., 1989; Strouthidis et al., 2006; Wollstein et al., 2005). Harwerth et al., for example, demonstrated in a population of 10 rhesus monkeys that SAP testing could not provide a useful estimate of ganglion cell losses at early stages of VF defects. Only in cases of more advanced glaucoma, visual field loss was directly related to ganglion cell loss (Harwerth et al., 1999). Similarly, Kerrigan-Baumrind et al. compared 17 eyes of 13 human glaucoma subjects post-mortem and reported that at least 35% of RGCs died before statistically significant abnormalities were seen on the corresponding VF tests (Kerrigan-Baumrind et al., 2000). Although future studies are needed to further characterize the structure-function relationship, early identification of glaucomatous structural damage is important for early diagnosis, management, and prevention of disease progression and further vision loss (Alencar et al., 2010; Ederer et al., 1994; Leske et al., 1999; Lim et al., 2012; Mansouri et al., 2011; Musch et al., 1999). Furthermore, although SAP is widely employed for the diagnosis, staging, and monitoring of the disease, diagnosis of glaucoma may require repeated testing (Katz et al., 1995; Spry et al., 2003).

To some extent, glaucoma diagnosis occurring after morphological changes in the RNFL can be attributed to poor resolution of current imaging modalities, including standard OCT, as their ability to detect very early abnormalities of the retinal microstructure is limited. Non-AO OCT devices, for example, lack the resolution required to obtain a cross-sectional profile of individual bundles of retinal nerve fibers as they traverse through the RNFL. Since early detection of glaucomatous changes is key, AO-OCT's increased ability to image microscopic subtle changes and variations of the RNFL at the preclinical stage underscores its potential as an invaluable asset to clinicians going forward for glaucoma detection and monitoring, especially given that RGC axonal losses in this retinal layer have been reported to precede in many cases ONH structural changes and vision loss as detectable by SAP (Sommer et al., 1977; Sommer et al., 1991). It is worth noting that current RNFL thickness parameters generated by OCT devices have good diagnostic accuracy, reproducibility (Mwanza et al., 2010), and can aid clinicians in differentiating healthy from glaucomatous eyes even in the early stages of the disease, and determine stages of disease severity (Mwanza et al., 2011; Mwanza et al., 2012; Wu et al., 2012; Akashi et al., 2013; Yang et al., 2015).

In contrast, thanks to its micrometric level resolution, AO-OCT devices can obtain a cross-sectional profile and 3D mapping of individual RNFL axon bundles *in-vivo* (Zawadzki et al., 2008; Cense et al., 2009b; Torti et al., 2009; Kocaoglu et al., 2011a; Kocaoglu et al., 2014b), differentiate these bundles from Müller cell septa and fibers, and permit an increased characterization of structural differences in the RNFL between healthy and glaucomatous eyes. Indeed, AO-OCT devices outperformed standard SD-OCT in terms of clarity of the microscopic retina, particularly the RNFL, and demonstrated reproducible measurements (Kocaoglu et al., 2011a). In addition, a moderate correlation between retinal nerve fiber bundle width and RNFL thickness has been shown in healthy and glaucomatous eyes (Takayama et al., 2012). As measured with AO-OCT, RNFL bundles appear to thin and separate as they approach the fovea.

Author Manuscript Author Manuscript Author Manuscript Author Manuscript

The increased ability to visualize and quantify these nerve fiber bundles, which have also been demonstrated in flood-illuminated ophthalmoscopes and SLO (Huang et al., 2012; Takayama et al., 2012, Ramaswamy et al. 2014), have allowed for examination of differences in the bundles themselves and the observation that RNFL bundles possess a discrete reflectivity pattern. One study imaged the RNFL with AO-OCT in four healthy subjects and reported that the RNFL bundles reflect two times more light than the surrounding tissue (Kocaoglu et al., 2011a). It is speculated that this could be related to increased cellular activity and an overall increased number of organelles (Brown, 2003; Huang et al., 2013; Wang et al., 2003a) and it is currently thought that reflectance intensity may decrease prior to losses in thickness (Huang et al., 2011; Zhang et al., 2011; van der Schoot et al., 2012). Ultimately, the added benefits of AO-OCT and its ability to construct 3D maps will likely permit earlier detection and improved monitoring of microstructures within the RNFL of patients with glaucoma.

2.3 Lamina cribrosa

As the presumed site of axonal injury in glaucoma, the LC may play a role in neuronal death seen in glaucoma. The LC provides mechanical support to optic nerve fibers within the deep optic disc region. Automated measurements of 3D LC microarchitecture showed good reproducibility (Nadler et al., 2014b) and holds the potential to serve as biomarkers for glaucoma damage. LC microarchitecture changes have been observed *in-vivo* with SS-OCT in glaucomatous eyes when compared with healthy eyes (Wang et al., 2013) and, using histological preparation, LC pore, shape and size have been correlated with the severity and progression of glaucoma (Miller and Quigley, 1987; Tezel et al., 2004). Additionally, the LC was noted in several OCT studies to displace posteriorly in glaucomatous eyes compared to age-matched healthy eyes (Kim et al., 2015; Sawada et al., 2015; Jung et al., 2016) and thinner LC was associated with glaucoma progression (Chung et al., 2015). Overall, the structural thinning, pore deformities and posterior displacement of the LC (Morgan-Davies et al., 2004), likely impede axoplasmic flow within the optic nerve fibers which will impair survival of RGCs (Burgoyne, 2011; Quigley, 2011). This could lead to RGC apoptosis, contributing to glaucoma development and progression.

As OCT and AO technology evolve, they continue to provide more accurate detection of LC deformation and enhance our understanding of the structural pathogenesis of glaucoma, including the role of the LC in glaucoma and glaucoma progression. Buried deep within the ONH, imaging the entirety of the LC structure is often obscured by vasculature, peripapillary sclera, and neural tissue, or viewing is obstructed by other reflective structures anterior in the ONH (Sigal et al., 2010). The improved resolution of AO-OCT to less than 5 μm has enabled very high quality images of the posterior pole and increased visualization of the LC microstructure (Figures 2 and 3) (Nadler et al., 2014b) and better spatial characterization of LC microstructure in healthy eyes (Nadler et al., 2014a) (Figure 4). It is likely that novel systems that pair AO with the deeper tissue penetration of SS-OCT (Jian et al., 2016) offer promise in the ongoing study of the LC. While the LC's role in glaucoma progression is yet to be fully determined, SS-OCT, SD-OCT, and AO-OCT have undoubtedly allowed for increased visualization of the LC microstructure and improve the current understanding of the LC and its microarchitecture (Figure 5), (Videos 1, 2, and 3).

Author Manuscript Author Manuscript Author Manuscript Author Manuscript

3. Multimodal imaging: combining AO-OCT with other modalities

3.1 Scanning laser ophthalmoscopy

AO-OCT technology has been successfully integrated into multimodal imaging devices that include AO-SLO. Since then, AO-SLO has demonstrated itself as a complementary adjunctive diagnostic tool to OCT. The modality's high transverse resolution and contrast allow for the identification of structural changes at the photoreceptor level associated with retinal pathology. Detailed visualization of the RNFL (Figure 6), for example, is now possible. When paired with AO-OCT, it is possible to visualize the impact of modest perimetric defects on the RNFL appearance - structural losses in RNFL visualized with AO-SLO correspond to RNFL thickness differences on OCT and the corresponding local VF defects on SAP.

Although AO-SLO allows for high transverse resolutions, the axial resolution is limited in comparison with OCT. In contrast to SLO and conventional microscopy (Drexler et al., 2015), OCT decouples the transverse and axial or depth resolutions, achieving very high axial image resolution that are independent of focusing conditions and numerical aperture of the optics of the eye itself. On the other hand, SLO's faster scanning speeds and direct measurements of back reflected light intensity allows for detection of both scattered and fluorescent photons from the tissue, making SLO very attractive for functional retinal imaging and allowing for higher fidelity en-face retinal images than AO-OCT. By detecting signals that OCT cannot, data acquired with AO-SLO can be complementary to OCT. With the added benefit of increased axial resolution provided by OCT, it is now possible to visualize contrast differences with AO-SLO in different retinal layers, such as the inner and outer segments and the external limiting membrane (Felberer et al., 2014). These dual SLO/OCT AO systems can also use SLO images as a reference to eliminate the effects of eye movements on the OCT image in order to resolve individual cells in different retinal layers, including photoreceptors and retinal pigment epithelium.

For visualization of the LC, AO-SLO by itself lacks the sensitivity and axial resolution afforded with OCT methods to adequately view the LC with depth. With AO-OCT, LC microarchitecture complexity as a function of depth can be visualized, such as the fine details of the delicate bifurcations and fenestrations of LC pores as they traverse the depth of the LC. On the other hand, AO-SLO has produced the highest resolution images of the LC surface structure ever obtained with ophthalmic imaging and significant changes in glaucomatous eyes have been observed in LC structural parameters in both primates and human subjects using AO-SLO (Sredar et al., 2013; Vilupuru et al., 2007). Given that AO ophthalmic systems in general are vulnerable to artifacts caused by eye drift and micro saccades because of the relatively small field size, AO-SLO/OCT multimodal systems could greatly benefit from supportive eye trackers (Zawadzki et al., 2005).

In addition, investigators have successfully implemented AO-SLO for the purpose of conducting functional assessments of the visual system, such as microperimetry (Tuten et al., 2012), while at the same time utilizing OCT to scan the retina to determine precisely where the stimulus fails to evoke a response. Microperimetry techniques have been described with AO that are able to measure light sensitivities of local retinal lesions and

Author Manuscript Author Manuscript Author Manuscript Author Manuscript

individual groups of cones (Makous et al., 2006; Harmening et al., 2014; Bruce et al., 2015; Wang et al., 2015). Locations in AO-SLO images that do not show the cone mosaic and also fail to show OCT reflections corresponding to the photoreceptor layer may still maintain cone function when observing physiologic responses to visual stimuli (Wang et al., 2015), challenging the notion that photoreceptor structures must be visible on AO-SLO imaging for the corresponding retinal location to retain function.

Functional testing at the cellular level with or without microperimetry, however, is currently challenging. Using both AO and OCT techniques, multiple animal studies have sought to identify biomarkers that correspond to retinal function in order to overcome this, specifically aiming to implement ocular imaging modalities to assess functional responses at the cellular level without the need for subjective responses. For example, one study used a flood-illumination AO-equipped retina camera to monitor changes in photoreceptor reflectance in response to visible stimuli (Jonnal et al., 2007). Most of the reflected light exiting an individual cone photoreceptor originates from the two ends of the outer segment: the connecting cilium and the posterior tip (Zhang et al., 2006). En-face AO modalities have demonstrated stimulus induced reflectance changes in the cone outer segment (Grieve and Roorda, 2008; Jonnal et al., 2010; Rha et al., 2009) with greater than 80% of cones activated after the application of a visible stimulus (Rha et al., 2009). In an AO-SLO device, photoreceptor response magnitude showed an average increase between 0% and 5% in the stimulated areas, with the most robust responses measured at a 3° peripheral location (Gri eve and Roorda, 2008). Such functional imaging may prove useful for examination of retinal function normal and diseased retinas.

Additionally, transversal scanning or en-face AO-OCT has also been integrated with SLO (Felberer et al., 2014), which provides information used for transverse motion correction in post-processing. In this case, aided by axial eye tracking, this device acquires volumes with high lateral and axial resolution and provided high resolution images of the photoreceptor mosaic. These systems are also useful for imaging the retinal vasculature, allowing for high resolution imaging of vessel walls and structures that may correspond to individual erythrocytes (Felberer et al., 2015).

3.2 Fundus cameras

Compact devices that combine AO-OCT with AO fundus cameras have also been demonstrated (Salas et al., 2016). Understandably, fundus cameras were the first imaging devices to implement AO technology in ophthalmology, as they employ simple optical principles involving little more than a camera capturing the light originating on the retina and emerging from the eye's optics to form an image on a light-sensitive film or charge coupled device. AO fundus cameras have since been used to image multiple structures in the eye, including photoreceptors (Lombardo et al., 2012), the RNFL (Ramaswamy et al., 2014) and retinal microvasculature (Popovic et al., 2011).

AO-OCT instruments alone have the disadvantage of having a smaller field of view in the imaging. The technology is somewhat restricted to imaging specific regions and identifying such regions can be challenging. AO-OCT multimodal systems that incorporate AO-fundus cameras or other modalities that provide a larger field of view are therefore advantageous,

Author Manuscript Author Manuscript Author Manuscript Author Manuscript

particularly for assisting with device alignment and proper registration of the smaller AO images. Standard wide-field OCT imaging has also been proposed for similar reasons. Additionally, the wider field of view facilitates with image comparison with the OCT: retinal features such as blood vessels, for example, can be easily identified. Conversely, again underscoring the major advantage of OCT in these systems, the depth information provided by the AO-OCT is important for full understanding of features seen on the AO-fundus images.

Due to the added benefit of depth information provided by the AO-OCT, this union in modalities has allowed researchers to examine microscopic retinal structures that were previously unable to be seen. This has been shown, for example, in the case of visualizing *in-vivo* the photoreceptor cone mosaic, which appear differently on AO-OCT when compared to AO-fundus images in systems that have combined both modalities (Zhang et al., 2006). This could be explained by the integration of OCT signals over a larger depth.

4. Future directions and conclusion

OCT has changed the face of glaucoma research and the ways that patients are diagnosed and followed in the clinic and remains a dynamic and evolving imaging modality. The technology has grown from TD-OCT devices to the improved SD-OCT, adapted novel image analysis and processing methods, and onto the newer SS-OCT and AO-OCT. Ongoing advances in OCT, such as faster scanning speeds, better visualization of retinal microstructure, and increased ability to assess functional aspects of these structures, should help elucidate new glaucoma diagnostic methods along with key pathogenic events and new treatment targets. Concurrently, AO technology is rapidly evolving alongside OCT and other ophthalmic imaging modalities.

Due to the key strengths of AO-OCT systems, the modality will have a major role in the ongoing study of structures related to glaucoma pathogenesis. AO-OCT imaging has a high potential in evaluating structural characteristics of the RNFL and identifying possible risk factors implicated in glaucomatous ONH damage. Additionally, the technology will aid the ongoing study and characterization of the structure-function relationship in glaucoma. Furthermore, because of its ability to capture very high resolution images at depth, AO-OCT can be particularly valuable in glaucoma for identifying early glaucomatous damages at the cellular level, detecting subtle RNFL, macular, or optic nerve head changes and abnormalities and monitoring for progression. And although the precise role of photoreceptors and changes in the photoreceptor layer in glaucoma is yet to be determined, this technology has proven to have the means to resolve this.

The combination of OCT with other complementary AO outfitted ophthalmic imaging modalities has certainly provided a more complete understanding of the various retinal locations under investigation. Furthermore, the integration of information from multiple modalities is often useful for new technologies, where there is far less experience in reading and interpretation of the images. Multimodal imaging, for example, has the advantage of providing complementary views of the retinal architecture and takes advantage of strengths of different imaging modalities. This provides the user with an added reference and

Author Manuscript Author Manuscript Author Manuscript Author Manuscript

additional information for the comparison and interpretation of images acquired with the new technology, yielding a more complete picture of the anatomy under investigation. Ultimately, the application of AO-OCT in this way has allowed for new discoveries related to glaucoma and hold promise for new insight in the future.

Supplementary Material

Refer to Web version on PubMed Central for supplementary material.

Acknowledgements

Supported in part by National Institutes of Health National Eye Institute R01-EY013178, (Bethesda, MD, USA), The Eye and Ear Foundation (Pittsburgh, PA, USA), and Research to Prevent Blindness (New York, NY, USA).

References

Akashi A, Kanamori A, Nakamura M, Fujihara M, Yamada Y, Negi A. Comparative assessment for the ability of Cirrus, RTVue, and 3D-OCT to diagnose glaucoma. Invest Ophthalmol Vis Sci. 2013; 54:4478–4484. [PubMed: 23737470]

Alencar LM, Zangwill LM, Weinreb RN, Bowd C, Sample PA, Girkin CA, Liebmann JM, Medeiros FA. A comparison of rates of change in neuroretinal rim area and retinal nerve fiber layer thickness in progressive glaucoma. Invest Ophthalmol Vis Sci. 2010; 51:3531–3539. [PubMed: 20207973]

Artal P, Guirao A, Berrio E, Williams DR. Compensation of corneal aberrations by the internal optics in the human eye. J Vis. 2001; 1:1–8. [PubMed: 12678609]

Artes PH, Chauhan BC. Longitudinal changes in the visual field and optic disc in glaucoma. Prog Retin Eye Res. 2005; 24:333–354. [PubMed: 15708832]

Bedggood P, Metha A. Variability in bleach kinetics and amount of photopigment between individual foveal cones. Invest Ophthalmol Vis Sci. 2012; 53:3673–3681. [PubMed: 22531694]

Brown A. Axonal transport of membranous and nonmembranous cargoes: a unified perspective. J Cell Biol. 2003; 160:817–821. [PubMed: 12642609]

Bruce KS, Harmening WM, Langston BR, Tuten WS, Roorda A, Sincich LC. Normal Perceptual Sensitivity Arising From Weakly Reflective Cone Photoreceptors. Invest Ophthalmol Vis Sci. 2015; 56:4431–4438. [PubMed: 26193919]

Buchi ER. Cell death in the rat retina after a pressure-induced ischaemia-reperfusion insult: an electron microscopic study. I. Ganglion cell layer and inner nuclear layer. Exp Eye Res. 1992; 55:605–613. [PubMed: 1483506]

Burgoyne CF. A biomechanical paradigm for axonal insult within the optic nerve head in aging and glaucoma. Exp Eye Res. 2011; 93:120–132. [PubMed: 20849846]

Burns SA, Tumbar R, Elsner AE, Ferguson D, Hammer DX. Large-field-of-view, modular, stabilized, adaptive-optics-based scanning laser ophthalmoscope. J Opt Soc Am A Opt Image Sci Vis. 2007; 24:1313–1326. [PubMed: 17429477]

Castejon-Mochon JF, Lopez-Gil N, Benito A, Artal P. Ocular wave-front aberration statistics in a normal young population. Vision Res. 2002; 42:1611–1617. [PubMed: 12079789]

Cense B, Gao W, Brown JM, Jones SM, Jonnal RS, Mujat M, Park BH, de Boer JF, Miller DT. Retinal imaging with polarization-sensitive optical coherence tomography and adaptive optics. Opt Express. 2009a; 17:21634–21651. [PubMed: 19997405]

Cense B, Koperda E, Brown JM, Kocaoglu OP, Gao W, Jonnal RS, Miller DT. Volumetric retinal imaging with ultrahigh-resolution spectral-domain optical coherence tomography and adaptive optics using two broadband light sources. Opt Express. 2009b; 17:4095–4111. [PubMed: 19259249]

Charman WN, Chateau N. The prospects for super-acuity: limits to visual performance after correction of monochromatic ocular aberration. Ophthalmic Physiol Opt. 2003; 23:479–493. [PubMed: 14622350]

Author Manuscript Author Manuscript Author Manuscript Author Manuscript

Chen Y, Ratnam K, Sundquist SM, Lujan B, Ayyagari R, Gudiseva VH, Roorda A, Duncan JL. Cone photoreceptor abnormalities correlate with vision loss in patients with Stargardt disease. Invest Ophthalmol Vis Sci. 2011; 52:3281–3292. [PubMed: 21296825]

Chinn SR, Swanson EA, Fujimoto JG. Optical coherence tomography using a frequency-tunable optical source. Opt Lett. 1997; 22:340–342. [PubMed: 18183195]

Choi SS, Doble N, Hardy JL, Jones SM, Keltner JL, Olivier SS, Werner JS. In vivo imaging of the photoreceptor mosaic in retinal dystrophies and correlations with visual function. Invest Ophthalmol Vis Sci. 2006; 47:2080–2092. [PubMed: 16639019]

Choi SS, Zawadzki RJ, Keltner JL, Werner JS. Changes in cellular structures revealed by ultra-high resolution retinal imaging in optic neuropathies. Invest Ophthalmol Vis Sci. 2008; 49:2103–2119. [PubMed: 18436843]

Choi SS, Zawadzki RJ, Lim MC, Brandt JD, Keltner JL, Doble N, Werner JS. Evidence of outer retinal changes in glaucoma patients as revealed by ultrahigh-resolution in vivo retinal imaging. Br J Ophthalmol. 2011; 95:131–141. [PubMed: 20956277]

Chung HS, Sung KR, Lee JY, Na JH. Lamina Cribrosa-Related Parameters Assessed by Optical Coherence Tomography for Prediction of Future Glaucoma Progression. Curr Eye Res. 2015:1–8.

Cooper RF, Dubis AM, Pavaskar A, Rha J, Dubra A, Carroll J. Spatial and temporal variation of rod photoreceptor reflectance in the human retina. Biomed Opt Express. 2011; 2:2577–2589. [PubMed: 21991550]

Dees EW, Dubra A, Baraas RC. Variability in parafoveal cone mosaic in normal trichromatic individuals. Biomed Opt Express. 2011; 2:1351–1358. [PubMed: 21559146]

Diaz-Santana L, Torti C, Munro I, Gasson P, Dainty C. Benefit of higher closed-loop bandwidths in ocular adaptive optics. Opt Express. 2003; 11:2597–2605. [PubMed: 19471373]

Donnelly WJ 3rd, Roorda A. Optimal pupil size in the human eye for axial resolution. J Opt Soc Am A Opt Image Sci Vis. 2003; 20:2010–2015. [PubMed: 14620328]

Dreher AW, Bille JF, Weinreb RN. Active optical depth resolution improvement of the laser tomographic scanner. Appl Opt. 1989; 28:804–808. [PubMed: 20548563]

Drexler, W., Chen, Y., Aguirre, AD., Považay, B., Unterhuber, A., Fujimoto, JG. Ultrahigh Resolution Optical Coherence Tomography. In: Drexler, W., Fujimoto, GJ., editors. Optical Coherence Tomography: Technology and Applications. Springer International Publishing, Cham; 2015. p. 277-318.

Dubra A, Sulai Y. Reflective afocal broadband adaptive optics scanning ophthalmoscope. Biomed Opt Express. 2011; 2:1757–1768. [PubMed: 21698035]

Dubra A, Sulai Y, Norris JL, Cooper RF, Dubis AM, Williams DR, Carroll J. Noninvasive imaging of the human rod photoreceptor mosaic using a confocal adaptive optics scanning ophthalmoscope. Biomed Opt Express. 2011; 2:1864–1876. [PubMed: 21750765]

Ederer F, Gaasterland DE, Sullivan EK, Investigators A. The Advanced Glaucoma Intervention Study (AGIS): 1. Study design and methods and baseline characteristics of study patients. Control Clin Trials. 1994; 15:299–325. [PubMed: 7956270]

Fazio DT, Heckenlively JR, Martin DA, Christensen RE. The electroretinogram in advanced open-angle glaucoma. Doc Ophthalmol. 1986; 63:45–54. [PubMed: 3732012]

Felberer F, Kroisamer JS, Baumann B, Zotter S, Schmidt-Erfurth U, Hitzenberger CK, Pircher M. Adaptive optics SLO/OCT for 3D imaging of human photoreceptors in vivo. Biomed Opt Express. 2014; 5:439–456. [PubMed: 24575339]

Felberer F, Rechenmacher M, Haindl R, Baumann B, Hitzenberger CK, Pircher M. Imaging of retinal vasculature using adaptive optics SLO/OCT. Biomed Opt Express. 2015; 6:1407–1418. [PubMed: 25909024]

Fercher AF, Mengedoht K, Werner W. Eye-length measurement by interferometry with partially coherent light. Opt Lett. 1988; 13:186–188. [PubMed: 19742022]

Fernandez E, Drexler W. Influence of ocular chromatic aberration and pupil size on transverse resolution in ophthalmic adaptive optics optical coherence tomography. Opt Express. 2005; 13:8184–8197. [PubMed: 19498848]

Author Manuscript Author Manuscript Author Manuscript Author Manuscript

Fernandez EJ, Hermann B, Povazay B, Unterhuber A, Sattmann H, Hofer B, Ahnelt PK, Drexler W. Ultrahigh resolution optical coherence tomography and pancorrection for cellular imaging of the living human retina. Opt Express. 2008; 16:11083–11094. [PubMed: 18648422]

Fernandez EJ, Povazay B, Hermann B, Unterhuber A, Sattmann H, Prieto PM, Leitgeb R, Ahnelt P, Artal P, Drexler W. Three-dimensional adaptive optics ultrahigh-resolution optical coherence tomography using a liquid crystal spatial light modulator. Vision Res. 2005; 45:3432–3444. [PubMed: 16249013]

Foster PJ, Buhrmann R, Quigley HA, Johnson GJ. The definition and classification of glaucoma in prevalence surveys. Br J Ophthalmol. 2002; 86:238–242. [PubMed: 11815354]

Garcia-Valenzuela E, Shareef S, Walsh J, Sharma SC. Programmed cell death of retinal ganglion cells during experimental glaucoma. Exp Eye Res. 1995; 61:33–44. [PubMed: 7556468]

Genead MA, Fishman GA, Rha J, Dubis AM, Bonci DM, Dubra A, Stone EM, Neitz M, Carroll J. Photoreceptor structure and function in patients with congenital achromatopsia. Invest Ophthalmol Vis Sci. 2011; 52:7298–7308. [PubMed: 21778272]

Girach, A., Sergott, RC. Optical Coherence Tomography. Springer; 2016.

Godara P, Dubis AM, Roorda A, Duncan JL, Carroll J. Adaptive optics retinal imaging: emerging clinical applications. Optom Vis Sci. 2010; 87:930–941. [PubMed: 21057346]

Gonzalez-Garcia AO, Vizzeri G, Bowd C, Medeiros FA, Zangwill LM, Weinreb RN. Reproducibility of RTVue retinal nerve fiber layer thickness and optic disc measurements and agreement with Stratus optical coherence tomography measurements. Am J Ophthalmol. 2009; 147:1067–1074. 1074, e1061. [PubMed: 19268891]

Grieve K, Roorda A. Intrinsic signals from human cone photoreceptors. Invest Ophthalmol Vis Sci. 2008; 49:713–719. [PubMed: 18235019]

Guirao A, Porter J, Williams DR, Cox IG. Calculated impact of higher-order monochromatic aberrations on retinal image quality in a population of human eyes. J Opt Soc Am A Opt Image Sci Vis. 2002; 19:620–628. [PubMed: 11876329]

Hammer DX, Ferguson RD, Mujat M, Patel A, Plumb E, Iftimia N, Chui TY, Akula JD, Fulton AB. Multimodal adaptive optics retinal imager: design and performance. J Opt Soc Am A Opt Image Sci Vis. 2012; 29:2598–2607. [PubMed: 23455909]

Hammer DX, Iftimia NV, Ferguson RD, Bigelow CE, Ustun TE, Barnaby AM, Fulton AB. Foveal fine structure in retinopathy of prematurity: an adaptive optics Fourier domain optical coherence tomography study. Invest Ophthalmol Vis Sci. 2008; 49:2061–2070. [PubMed: 18223243]

Harmening WM, Tuten WS, Roorda A, Sincich LC. Mapping the perceptual grain of the human retina. J Neurosci. 2014; 34:5667–5677. [PubMed: 24741057]

Harwerth RS, Carter-Dawson L, Shen F, Smith EL 3rd, Crawford ML. Ganglion cell losses underlying visual field defects from experimental glaucoma. Invest Ophthalmol Vis Sci. 1999; 40:2242–2250. [PubMed: 10476789]

He Z, Bui BV, Vingrys AJ. The rate of functional recovery from acute IOP elevation. Invest Ophthalmol Vis Sci. 2006; 47:4872–4880. [PubMed: 17065501]

Hermann B, Fernandez EJ, Unterhuber A, Sattmann H, Fercher AF, Drexler W, Prieto PM, Artal P. Adaptive-optics ultrahigh-resolution optical coherence tomography. Opt Lett. 2004; 29:2142–2144. [PubMed: 15460883]

Hofer H, Artal P, Singer B, Aragon JL, Williams DR. Dynamics of the eye's wave aberration. J Opt Soc Am A Opt Image Sci Vis. 2001; 18:497–506. [PubMed: 11265680]

Holopigian K, Seiple W, Mayron C, Koty R, Lorenzo M. Electrophysiological and psychophysical flicker sensitivity in patients with primary open-angle glaucoma and ocular hypertension. Invest Ophthalmol Vis Sci. 1990; 31:1863–1868. [PubMed: 2211032]

Hougaard JL, Heijl A, Bengtsson B. Glaucoma detection by Stratus OCT. J Glaucoma. 2007a; 16:302–306. [PubMed: 17438424]

Hougaard JL, Heijl A, Bengtsson B. Glaucoma detection using different Stratus optical coherence tomography protocols. Acta Ophthalmol Scand. 2007b; 85:251–256. [PubMed: 17343690]

Huang D, Swanson EA, Lin CP, Schuman JS, Stinson WG, Chang W, Hee MR, Flotte T, Gregory K, Puliafito CA, et al. Optical coherence tomography. Science. 1991; 254:1178–1181. [PubMed: 1957169]

Author Manuscript Author Manuscript Author Manuscript Author Manuscript

Huang G, Qi X, Chui TY, Zhong Z, Burns SA. A clinical planning module for adaptive optics SLO imaging. Optom Vis Sci. 2012; 89:593–601. [PubMed: 22488269]

Huang XR, Knighton RW, Zhou Y, Zhao XP. Reflectance speckle of retinal nerve fiber layer reveals axonal activity. Invest Ophthalmol Vis Sci. 2013; 54:2616–2623. [PubMed: 23532525]

Huang XR, Zhou Y, Kong W, Knighton RW. Reflectance decreases before thickness changes in the retinal nerve fiber layer in glaucomatous retinas. Invest Ophthalmol Vis Sci. 2011; 52:6737–6742. [PubMed: 21730345]

Iliev ME, Meyenberg A, Garweg JG. Morphometric assessment of normal, suspect and glaucomatous optic discs with Stratus OCT and HRT II. Eye (Lond). 2006; 20:1288–1299. [PubMed: 16179933]

Ishikawa H, Gabriele ML, Wollstein G, Ferguson RD, Hammer DX, Paunescu LA, Beaton SA, Schuman JS. Retinal nerve fiber layer assessment using optical coherence tomography with active optic nerve head tracking. Invest Ophthalmol Vis Sci. 2006; 47:964–967. [PubMed: 16505030]

Jian Y, Lee S, Ju MJ, Heisler M, Ding W, Zawadzki RJ, Bonora S, Sarunic MV. Lens-based wavefront sensorless adaptive optics swept source OCT. Sci Rep. 2016; 6:27620. [PubMed: 27278853]

Jonnal RS, Besecker JR, Derby JC, Kocaoglu OP, Cense B, Gao W, Wang Q, Miller DT. Imaging outer segment renewal in living human cone photoreceptors. Opt Express. 2010; 18:5257–5270. [PubMed: 20389538]

Jonnal RS, Kocaoglu OP, Wang Q, Lee S, Miller DT. Phase-sensitive imaging of the outer retina using optical coherence tomography and adaptive optics. Biomed Opt Express. 2012; 3:104–124. [PubMed: 22254172]

Jonnal RS, Kocaoglu OP, Zawadzki RJ, Liu Z, Miller DT, Werner JS. A Review of Adaptive Optics Optical Coherence Tomography: Technical Advances, Scientific Applications, and the Future. Invest Ophthalmol Vis Sci. 2016; 57:OCT51–68. [PubMed: 27409507]

Jonnal RS, Rha J, Zhang Y, Cense B, Gao W, Miller DT. In vivo functional imaging of human cone photoreceptors. Opt Express. 2007; 15:16141–16160.

Jung KI, Jeon S, Park CK. Lamina Cribrosa Depth is Associated With the Cup-to-Disc Ratio in Eyes With Large Optic Disc Cupping and Cup-to-Disc Ratio Asymmetry. J Glaucoma. 2016

Katz J, Quigley HA, Sommer A. Repeatability of the Glaucoma Hemifield Test in automated perimetry. Invest Ophthalmol Vis Sci. 1995; 36:1658–1664. [PubMed: 7601645]

Kendell KR, Quigley HA, Kerrigan LA, Pease ME, Quigley EN. Primary open-angle glaucoma is not associated with photoreceptor loss. Invest Ophthalmol Vis Sci. 1995; 36:200–205. [PubMed: 7822147]

Kerrigan-Baumrind LA, Quigley HA, Pease ME, Kerrigan DF, Mitchell RS. Number of ganglion cells in glaucoma eyes compared with threshold visual field tests in the same persons. Invest Ophthalmol Vis Sci. 2000; 41:741–748. [PubMed: 10711689]

Kim JS, Ishikawa H, Gabriele ML, Wollstein G, Bilonick RA, Kagemann L, Fujimoto JG, Schuman JS. Retinal nerve fiber layer thickness measurement comparability between time domain optical coherence tomography (OCT) and spectral domain OCT. Invest Ophthalmol Vis Sci. 2010; 51:896–902. [PubMed: 19737886]

Kim JS, Ishikawa H, Sung KR, Xu J, Wollstein G, Bilonick RA, Gabriele ML, Kagemann L, Duker JS, Fujimoto JG, Schuman JS. Retinal nerve fibre layer thickness measurement reproducibility improved with spectral domain optical coherence tomography. Br J Ophthalmol. 2009; 93:1057–1063. [PubMed: 19429591]

Kim YW, Kim DW, Jeoung JW, Kim DM, Park KH. Peripheral lamina cribrosa depth in primary open-angle glaucoma: a swept-source optical coherence tomography study of lamina cribrosa. Eye (Lond). 2015; 29:1368–1374. [PubMed: 26293139]

Knight OJ, Chang RT, Feuer WJ, Budenz DL. Comparison of retinal nerve fiber layer measurements using time domain and spectral domain optical coherent tomography. Ophthalmology. 2009; 116:1271–1277. [PubMed: 19395086]

Kocaoglu OP, Cense B, Jonnal RS, Wang Q, Lee S, Gao W, Miller DT. Imaging retinal nerve fiber bundles using optical coherence tomography with adaptive optics. Vision Res. 2011a; 51:1835–1844. [PubMed: 21722662]

Author Manuscript Author Manuscript Author Manuscript Author Manuscript

Kocaoglu OP, Ferguson RD, Jonnal RS, Liu Z, Wang Q, Hammer DX, Miller DT. Adaptive optics optical coherence tomography with dynamic retinal tracking. Biomed Opt Express. 2014a; 5:2262–2284. [PubMed: 25071963]

Kocaoglu, OP., Lee, S., Jonnal, RS., Wang, Q., Herde, AE., Besecker, J., Gao, W., Miller, DT. 3D imaging of cone photoreceptors over extended time periods using optical coherence tomography with adaptive optics. 2011b. p. 78850C-78850C-78856.

Kocaoglu OP, Lee S, Jonnal RS, Wang Q, Herde AE, Derby JC, Gao W, Miller DT. Imaging cone photoreceptors in three dimensions and in time using ultrahigh resolution optical coherence tomography with adaptive optics. Biomed Opt Express. 2011c; 2:748–763. [PubMed: 21483600]

Kocaoglu OP, Turner TL, Liu Z, Miller DT. Adaptive optics optical coherence tomography at 1 MHz. Biomed Opt Express. 2014b; 5:4186–4200. [PubMed: 25574431]

Kong YX, Crowston JG, Vingrys AJ, Trounce IA, Bui VB. Functional changes in the retina during and after acute intraocular pressure elevation in mice. Invest Ophthalmol Vis Sci. 2009; 50:5732–5740. [PubMed: 19643960]

Kuang TM, Zhang C, Zangwill LM, Weinreb RN, Medeiros FA. Estimating Lead Time Gained by Optical Coherence Tomography in Detecting Glaucoma before Development of Visual Field Defects. Ophthalmology. 2015; 122:2002–2009. [PubMed: 26198809]

Kurokawa K, Tamada D, Makita S, Yasuno Y. Adaptive optics retinal scanner for one-micrometer light source. Opt Express. 2010; 18:1406–1418. [PubMed: 20173968]

Lee EJ, Kim TW, Park KH, Seong M, Kim H, Kim DM. Ability of Stratus OCT to detect progressive retinal nerve fiber layer atrophy in glaucoma. Invest Ophthalmol Vis Sci. 2009; 50:662–668. [PubMed: 18824734]

Leite MT, Rao HL, Zangwill LM, Weinreb RN, Medeiros FA. Comparison of the diagnostic accuracies of the Spectralis, Cirrus, and RTVue optical coherence tomography devices in glaucoma. Ophthalmology. 2011; 118:1334–1339. [PubMed: 21377735]

Leitgeb R, Hitzenberger C, Fercher A. Performance of fourier domain vs. time domain optical coherence tomography. Opt Express. 2003; 11:889–894. [PubMed: 19461802]

Leske MC, Heijl A, Hyman L, Bengtsson B. Early Manifest Glaucoma Trial: design and baseline data. Ophthalmology. 1999; 106:2144–2153. [PubMed: 10571351]

Leung CK, Cheung CY, Weinreb RN, Qiu Q, Liu S, Li H, Xu G, Fan N, Huang L, Pang CP, Lam DS. Retinal nerve fiber layer imaging with spectral-domain optical coherence tomography: a variability and diagnostic performance study. Ophthalmology. 2009; 116:1257–1263. 1263, e1251–1252. [PubMed: 19464061]

Leung CK, Lam S, Weinreb RN, Liu S, Ye C, Liu L, He J, Lai GW, Li T, Lam DS. Retinal nerve fiber layer imaging with spectral-domain optical coherence tomography: analysis of the retinal nerve fiber layer map for glaucoma detection. Ophthalmology. 2010; 117:1684–1691. [PubMed: 20663563]

Leung CK, Liu S, Weinreb RN, Lai G, Ye C, Cheung CY, Pang CP, Tse KK, Lam DS. Evaluation of retinal nerve fiber layer progression in glaucoma a prospective analysis with neuroretinal rim and visual field progression. Ophthalmology. 2011; 118:1551–1557. [PubMed: 21529958]

Liang J, Grimm B, Goelz S, Bille JF. Objective measurement of wave aberrations of the human eye with the use of a Hartmann-Shack wave-front sensor. J Opt Soc Am A Opt Image Sci Vis. 1994; 11:1949–1957. [PubMed: 8071736]

Liang J, Williams DR, Miller DT. Supernormal vision and high-resolution retinal imaging through adaptive optics. J Opt Soc Am A Opt Image Sci Vis. 1997; 14:2884–2892. [PubMed: 9379246]

Lim TC, Chattopadhyay S, Acharya UR. A survey and comparative study on the instruments for glaucoma detection. Med Eng Phys. 2012; 34:129–139. [PubMed: 21862378]

Lombardo M, Lombardo G. New methods and techniques for sensing the wave aberrations of human eyes. Clin Exp Optom. 2009; 92:176–186. [PubMed: 19243390]

Lombardo M, Lombardo G, Ducoli P, Serrao S. Adaptive optics photoreceptor imaging. Ophthalmology. 2012; 119:1498–1498. e1492.

Lombardo M, Serrao S, Devaney N, Parravano M, Lombardo G. Adaptive optics technology for high-resolution retinal imaging. Sensors (Basel). 2013; 13:334–366.

Author Manuscript Author Manuscript Author Manuscript Author Manuscript

Makous W, Carroll J, Wolfing JI, Lin J, Christie N, Williams DR. Retinal microscotomas revealed with adaptive-optics microflashes. Invest Ophthalmol Vis Sci. 2006; 47:4160–4167. [PubMed: 16936137]

Manassakorn A, Nouri-Mahdavi K, Caprioli J. Comparison of retinal nerve fiber layer thickness and optic disk algorithms with optical coherence tomography to detect glaucoma. Am J Ophthalmol. 2006; 141:105–115. [PubMed: 16386983]

Mansouri K, Leite MT, Medeiros FA, Leung CK, Weinreb RN. Assessment of rates of structural change in glaucoma using imaging technologies. Eye (Lond). 2011; 25:269–277. [PubMed: 21212798]

Mansouri K, Medeiros FA, Marchase N, Tatham AJ, Auerbach D, Weinreb RN. Assessment of choroidal thickness and volume during the water drinking test by swept-source optical coherence tomography. Ophthalmology. 2013a; 120:2508–2516. [PubMed: 24021895]

Mansouri K, Nuyen B, R NW. Improved visualization of deep ocular structures in glaucoma using high penetration optical coherence tomography. Expert Rev Med Devices. 2013b; 10:621–628. [PubMed: 23972075]

Martin JA, Roorda A. Pulsatility of parafoveal capillary leukocytes. Exp Eye Res. 2009; 88:356–360. [PubMed: 18708051]

Medeiros FA, Alencar LM, Zangwill LM, Bowd C, Sample PA, Weinreb RN. Prediction of functional loss in glaucoma from progressive optic disc damage. Arch Ophthalmol. 2009a; 127:1250–1256. [PubMed: 19822839]

Medeiros FA, Lisboa R, Weinreb RN, Liebmann JM, Girkin C, Zangwill LM. Retinal ganglion cell count estimates associated with early development of visual field defects in glaucoma. Ophthalmology. 2013; 120:736–744. [PubMed: 23246120]

Medeiros FA, Zangwill LM, Alencar LM, Bowd C, Sample PA, Susanna R Jr. Weinreb RN. Detection of glaucoma progression with stratus OCT retinal nerve fiber layer, optic nerve head, and macular thickness measurements. Invest Ophthalmol Vis Sci. 2009b; 50:5741–5748. [PubMed: 19815731]

Medeiros FA, Zangwill LM, Bowd C, Vessani RM, Susanna R Jr. Weinreb RN. Evaluation of retinal nerve fiber layer, optic nerve head, and macular thickness measurements for glaucoma detection using optical coherence tomography. Am J Ophthalmol. 2005; 139:44–55. [PubMed: 15652827]

Medeiros FA, Zangwill LM, Bowd C, Weinreb RN. Comparison of the GDx VCC scanning laser polarimeter, HRT II confocal scanning laser ophthalmoscope, and stratus OCT optical coherence tomograph for the detection of glaucoma. Arch Ophthalmol. 2004; 122:827–837. [PubMed: 15197057]

Menke MN, Dabov S, Knecht P, Sturm V. Reproducibility of retinal thickness measurements in healthy subjects using spectralis optical coherence tomography. Am J Ophthalmol. 2009; 147:467–472. [PubMed: 19026403]

Merino D, Dainty C, Bradu A, Podoleanu AG. Adaptive optics enhanced simultaneous en-face optical coherence tomography and scanning laser ophthalmoscopy. Opt Express. 2006; 14:3345–3353. [PubMed: 19516479]

Miglior S, Zeyen T, Pfeiffer N, Cunha-Vaz J, Torri V, Adamsons I, European Glaucoma Prevention Study, G. Results of the European Glaucoma Prevention Study. Ophthalmology. 2005; 112:366–375. [PubMed: 15745761]

Miller, DT., Qu, J., Jonnal, RS., Thorn, KE. Coherence gating and adaptive optics in the eye. 2003. p. 65-72.

Miller DT, Williams DR, Morris GM, Liang J. Images of cone photoreceptors in the living human eye. Vision Res. 1996; 36:1067–1079. [PubMed: 8762712]

Miller KM, Quigley HA. Comparison of optic disc features in low-tension and typical open-angle glaucoma. Ophthalmic Surg. 1987; 18:882–889. [PubMed: 3444599]

Morgan-Davies J, Taylor N, Hill AR, Aspinall P, O'Brien CJ, Azuara-Blanco A. Three dimensional analysis of the lamina cribrosa in glaucoma. Br J Ophthalmol. 2004; 88:1299–1304. [PubMed: 15377555]

Author Manuscript Author Manuscript Author Manuscript Author Manuscript

Musch DC, Lichter PR, Guire KE, Standardi CL. The Collaborative Initial Glaucoma Treatment Study: study design, methods, and baseline characteristics of enrolled patients. Ophthalmology. 1999; 106:653–662. [PubMed: 10201583]

Mwanza JC, Budenz DL. Optical coherence tomography platforms and parameters for glaucoma diagnosis and progression. Curr Opin Ophthalmol. 2015

Mwanza JC, Chang RT, Budenz DL, Durbin MK, Gendy MG, Shi W, Feuer WJ. Reproducibility of peripapillary retinal nerve fiber layer thickness and optic nerve head parameters measured with cirrus HD-OCT in glaucomatous eyes. Invest Ophthalmol Vis Sci. 2010; 51:5724–5730. [PubMed: 20574014]

Mwanza JC, Durbin MK, Budenz DL, Sayyad FE, Chang RT, Neelakantan A, Godfrey DG, Carter R, Crandall AS. Glaucoma diagnostic accuracy of ganglion cell-inner plexiform layer thickness: comparison with nerve fiber layer and optic nerve head. Ophthalmology. 2012; 119:1151–1158. [PubMed: 22365056]

Mwanza JC, Oakley JD, Budenz DL, Anderson DR, Cirrus Optical Coherence Tomography Normative Database Study, G. Ability of cirrus HD-OCT optic nerve head parameters to discriminate normal from glaucomatous eyes. Ophthalmology. 2011; 118:241–248. e241. [PubMed: 20920824]

Nadler Z, Wang B, Schuman JS, Ferguson RD, Patel A, Hammer DX, Bilonick RA, Ishikawa H, Kagemann L, Sigal IA, Wollstein G. In vivo three-dimensional characterization of the healthy human lamina cribrosa with adaptive optics spectral-domain optical coherence tomography. Invest Ophthalmol Vis Sci. 2014a; 55:6459–6466. [PubMed: 25228539]

Nadler Z, Wang B, Wollstein G, Nevins JE, Ishikawa H, Bilonick R, Kagemann L, Sigal IA, Ferguson RD, Patel A, Hammer DX, Schuman JS. Repeatability of in vivo 3D lamina cribrosa microarchitecture using adaptive optics spectral domain optical coherence tomography. Biomed Opt Express. 2014b; 5:1114–1123. [PubMed: 24761293]

Naithani P, Sihota R, Sony P, Dada T, Gupta V, Kondal D, Pandey RM. Evaluation of optical coherence tomography and heidelberg retinal tomography parameters in detecting early and moderate glaucoma. Invest Ophthalmol Vis Sci. 2007; 48:3138–3145. [PubMed: 17591883]

Nirmaier T, Pudasaini G, Bille J. Very fast wave-front measurements at the human eye with a custom CMOS-based Hartmann-Shack sensor. Opt Express. 2003; 11:2704–2716. [PubMed: 19471385]

Nork TM, Ver Hoeve JN, Poulsen GL, Nickells RW, Davis MD, Weber AJ, Vaegan, Sarks SH, Lemley HL, Millecchia LL. Swelling and loss of photoreceptors in chronic human and experimental glaucomas. Arch Ophthalmol. 2000; 118:235–245. [PubMed: 10676789]

Nouri-Mahdavi K, Nikkhou K, Hoffman DC, Law SK, Caprioli J. Detection of early glaucoma with optical coherence tomography (StratusOCT). J Glaucoma. 2008; 17:183–188. [PubMed: 18414102]

Odom JV, Feghali JG, Jin JC, Weinstein GW. Visual function deficits in glaucoma. Electroretinogram pattern and luminance nonlinearities. Arch Ophthalmol. 1990; 108:222–227. [PubMed: 2302106]

Ortega Jde L, Kakati B, Girkin CA. Artifacts on the optic nerve head analysis of the optical coherence tomography in glaucomatous and nonglaucomatous eyes. J Glaucoma. 2009; 18:186–191. [PubMed: 19295369]

Panda S, Jonas JB. Decreased photoreceptor count in human eyes with secondary angle-closure glaucoma. Invest Ophthalmol Vis Sci. 1992; 33:2532–2536. [PubMed: 1634350]

Parikh RS, Parikh S, Sekhar GC, Kumar RS, Prabakaran S, Babu JG, Thomas R. Diagnostic capability of optical coherence tomography (Stratus OCT 3) in early glaucoma. Ophthalmology. 2007; 114:2238–2243. [PubMed: 17561260]

Park HY, Shin HY, Park CK. Imaging the posterior segment of the eye using swept-source optical coherence tomography in myopic glaucoma eyes: comparison with enhanced-depth imaging. Am J Ophthalmol. 2014; 157:550–557. [PubMed: 24239773]

Park SB, Sung KR, Kang SY, Kim KR, Kook MS. Comparison of glaucoma diagnostic Capabilities of Cirrus HD and Stratus optical coherence tomography. Arch Ophthalmol. 2009; 127:1603–1609. [PubMed: 20008715]

Author Manuscript Author Manuscript Author Manuscript Author Manuscript

Pierro L, Gagliardi M, Iuliano L, Ambrosi A, Bandello F. Retinal nerve fiber layer thickness reproducibility using seven different OCT instruments. Invest Ophthalmol Vis Sci. 2012; 53:5912–5920. [PubMed: 22871835]

Platt BC, Shack R. History and principles of Shack-Hartmann wavefront sensing. J Refract Surg. 2001; 17:S573–577. [PubMed: 11583233]

Poinoosawmy D, Nagasubramanian S, Gloster J. Colour vision in patients with chronic simple glaucoma and ocular hypertension. Br J Ophthalmol. 1980; 64:852–857. [PubMed: 7426556]

Pokorny J, Smith VC. Eye disease and color defects. Vision Res. 1986; 26:1573–1584. [PubMed: 3303675]

Popovic Z, Knutsson P, Thaung J, Owner-Petersen M, Sjostrand J. Noninvasive imaging of human foveal capillary network using dual-conjugate adaptive optics. Invest Ophthalmol Vis Sci. 2011; 52:2649–2655. [PubMed: 21228372]

Porter J, Guirao A, Cox IG, Williams DR. Monochromatic aberrations of the human eye in a large population. J Opt Soc Am A Opt Image Sci Vis. 2001; 18:1793–1803. [PubMed: 11488483]

Porter, J., Queener, H., Lin, J., Thorn, K., Awwal, AAS. Adaptive Optics for Vision Science: Principles, Practices, Design and Applications. Wiley; 2006.

Puliafito CA. Optical coherence tomography: 20 years after. Ophthalmic Surg Lasers Imaging. 2010; 41(Suppl):S5. [PubMed: 21117600]

Puliafito CA, Hee MR, Lin CP, Reichel E, Schuman JS, Duker JS, Izatt JA, Swanson EA, Fujimoto JG. Imaging of macular diseases with optical coherence tomography. Ophthalmology. 1995; 102:217–229. [PubMed: 7862410]

Quigley HA. Glaucoma. Lancet. 2011; 377:1367–1377. [PubMed: 21453963]

Quigley HA, Broman AT. The number of people with glaucoma worldwide in 2010 and 2020. Br J Ophthalmol. 2006; 90:262–267. [PubMed: 16488940]

Quigley HA, Dunkelberger GR, Green WR. Retinal ganglion cell atrophy correlated with automated perimetry in human eyes with glaucoma. Am J Ophthalmol. 1989; 107:453–464. [PubMed: 2712129]

Quigley HA, Katz J, Derick RJ, Gilbert D, Sommer A. An evaluation of optic disc and nerve fiber layer examinations in monitoring progression of early glaucoma damage. Ophthalmology. 1992; 99:19–28. [PubMed: 1741133]

Quigley HA, Nickells RW, Kerrigan LA, Pease ME, Thibault DJ, Zack DJ. Retinal ganglion cell death in experimental glaucoma and after axotomy occurs by apoptosis. Invest Ophthalmol Vis Sci. 1995; 36:774–786. [PubMed: 7706025]

Ramaswamy G, Lombardo M, Devaney N. Registration of adaptive optics corrected retinal nerve fiber layer (RNFL) images. Biomed Opt Express. 2014; 5:1941–1951. [PubMed: 24940551]

Rao HL, Zangwill LM, Weinreb RN, Sample PA, Alencar LM, Medeiros FA. Comparison of different spectral domain optical coherence tomography scanning areas for glaucoma diagnosis. Ophthalmology. 2010; 117:1692–1699. 1699, e1691. [PubMed: 20493529]

Rha J, Jonnal RS, Thorn KE, Qu J, Zhang Y, Miller DT. Adaptive optics flood-illumination camera for high speed retinal imaging. Opt Express. 2006; 14:4552–4569. [PubMed: 19516608]

Rha J, Schroeder B, Godara P, Carroll J. Variable optical activation of human cone photoreceptors visualized using a short coherence light source. Opt Lett. 2009; 34:3782–3784. [PubMed: 20016612]

Roorda A, Romero-Borja F, Donnelly W Iii, Queener H, Hebert T, Campbell M. Adaptive optics scanning laser ophthalmoscopy. Opt Express. 2002; 10:405–412. [PubMed: 19436374]

Salas M, Drexler W, Levecq X, Lamory B, Ritter M, Prager S, Hafner J, Schmidt-Erfurth U, Pircher M. Multi-modal adaptive optics system including fundus photography and optical coherence tomography for the clinical setting. Biomed Opt Express. 2016; 7:1783–1796. [PubMed: 27231621]

Salmon TO, van de Pol C. Normal-eye Zernike coefficients and root-mean-square wavefront errors. J Cataract Refract Surg. 2006; 32:2064–2074. [PubMed: 17137985]

Sawada Y, Hangai M, Murata K, Ishikawa M, Yoshitomi T. Lamina Cribrosa Depth Variation Measured by Spectral-Domain Optical Coherence Tomography Within and Between Four

Author Manuscript Author Manuscript Author Manuscript Author Manuscript

Glaucomatous Optic Disc Phenotypes. Invest Ophthalmol Vis Sci. 2015; 56:5777–5784. [PubMed: 26325416]

Schmoll T, Singh AS, Blatter C, Schriefl S, Ahlers C, Schmidt-Erfurth U, Leitgeb RA. Imaging of the parafoveal capillary network and its integrity analysis using fractal dimension. Biomed Opt Express. 2011; 2:1159–1168. [PubMed: 21559128]

Schuman JS. Spectral domain optical coherence tomography for glaucoma (an AOS thesis). Trans Am Ophthalmol Soc. 2008; 106:426–458. [PubMed: 19277249]

Schuman JS, Hee MR, Arya AV, Pedut-Kloizman T, Puliafito CA, Fujimoto JG, Swanson EA. Optical coherence tomography: a new tool for glaucoma diagnosis. Curr Opin Ophthalmol. 1995; 6:89–95. [PubMed: 10150863]

Schuman JS, Pedut-Kloizman T, Hertzmark E, Hee MR, Wilkins JR, Coker JG, Puliafito CA, Fujimoto JG, Swanson EA. Reproducibility of nerve fiber layer thickness measurements using optical coherence tomography. Ophthalmology. 1996; 103:1889–1898. [PubMed: 8942887]

Sehi M, Grewal DS, Sheets CW, Greenfield DS. Diagnostic ability of Fourier-domain vs time-domain optical coherence tomography for glaucoma detection. Am J Ophthalmol. 2009; 148:597–605. [PubMed: 19589493]

Sigal IA, Flanagan JG, Tertinegg I, Ethier CR. 3D morphometry of the human optic nerve head. Exp Eye Res. 2010; 90:70–80. [PubMed: 19772858]

Sommer A, Katz J, Quigley HA, Miller NR, Robin AL, Richter RC, Witt KA. Clinically detectable nerve fiber atrophy precedes the onset of glaucomatous field loss. Arch Ophthalmol. 1991; 109:77–83. [PubMed: 1987954]

Sommer A, Miller NR, Pollack I, Maumenee AE, George T. The nerve fiber layer in the diagnosis of glaucoma. Arch Ophthalmol. 1977; 95:2149–2156. [PubMed: 588106]

Spry PG, Johnson CA, McKendrick AM, Turpin A. Measurement error of visual field tests in glaucoma. Br J Ophthalmol. 2003; 87:107–112. [PubMed: 12488273]

Sredar N, Ivers KM, Queener HM, Zouridakis G, Porter J. 3D modeling to characterize lamina cribrosa surface and pore geometries using in vivo images from normal and glaucomatous eyes. Biomed Opt Express. 2013; 4:1153–1165. [PubMed: 23847739]

Strouthidis NG, Scott A, Peter NM, Garway-Heath DF. Optic disc and visual field progression in ocular hypertensive subjects: detection rates, specificity, and agreement. Invest Ophthalmol Vis Sci. 2006; 47:2904–2910. [PubMed: 16799032]

Sun D, Bui BV, Vingrys AJ, Kalloniatis M. Alterations in photoreceptor-bipolar cell signaling following ischemia/reperfusion in the rat retina. J Comp Neurol. 2007; 505:131–146. [PubMed: 17729268]

Sung KR, Kim JS, Wollstein G, Folio L, Kook MS, Schuman JS. Imaging of the retinal nerve fibre layer with spectral domain optical coherence tomography for glaucoma diagnosis. Br J Ophthalmol. 2011; 95:909–914. [PubMed: 21030413]

Takayama K, Hangai M, Kimura Y, Morooka S, Nukada M, Akagi T, Ikeda HO, Matsumoto A, Yoshimura N. Three-dimensional imaging of lamina cribrosa defects in glaucoma using swept-source optical coherence tomography. Invest Ophthalmol Vis Sci. 2013; 54:4798–4807. [PubMed: 23778878]

Takayama K, Ooto S, Hangai M, Arakawa N, Oshima S, Shibata N, Hanebuchi M, Inoue T, Yoshimura N. High-resolution imaging of the retinal nerve fiber layer in normal eyes using adaptive optics scanning laser ophthalmoscopy. PLoS One. 2012; 7:e33158. [PubMed: 22427978]

Talcott KE, Ratnam K, Sundquist SM, Lucero AS, Lujan BJ, Tao W, Porco TC, Roorda A, Duncan JL. Longitudinal study of cone photoreceptors during retinal degeneration and in response to ciliary neurotrophic factor treatment. Invest Ophthalmol Vis Sci. 2011; 52:2219–2226. [PubMed: 21087953]

Tam J, Martin JA, Roorda A. Noninvasive visualization and analysis of parafoveal capillaries in humans. Invest Ophthalmol Vis Sci. 2010; 51:1691–1698. [PubMed: 19907024]

Tam J, Tiruveedhula P, Roorda A. Characterization of single-file flow through human retinal parafoveal capillaries using an adaptive optics scanning laser ophthalmoscope. Biomed Opt Express. 2011; 2:781–793. [PubMed: 21483603]

Author Manuscript Author Manuscript Author Manuscript Author Manuscript

Tezel G, Trinkaus K, Wax MB. Alterations in the morphology of lamina cribrosa pores in glaucomatous eyes. Br J Ophthalmol. 2004; 88:251–256. [PubMed: 14736786]

Thibos LN. The prospects for perfect vision. J Refract Surg. 2000; 16:S540–546. [PubMed: 11019868]

Thibos LN, Bradley A, Hong X. A statistical model of the aberration structure of normal, well-corrected eyes. Ophthalmic Physiol Opt. 2002a; 22:427–433. [PubMed: 12358314]

Thibos LN, Hong X, Bradley A, Cheng X. Statistical variation of aberration structure and image quality in a normal population of healthy eyes. J Opt Soc Am A Opt Image Sci Vis. 2002b; 19:2329–2348. [PubMed: 12469728]

Tojo N, Nakamura T, Fuchizawa C, Oiwake T, Hayashi A. Adaptive optics fundus images of cone photoreceptors in the macula of patients with retinitis pigmentosa. Clin Ophthalmol. 2013; 7:203–210. [PubMed: 23378739]

Torti C, Povazay B, Hofer B, Unterhuber A, Carroll J, Ahnelt PK, Drexler W. Adaptive optics optical coherence tomography at 120,000 depth scans/s for noninvasive cellular phenotyping of the living human retina. Opt Express. 2009; 17:19382–19400. [PubMed: 19997159]

Tuten WS, Tiruveedhula P, Roorda A. Adaptive optics scanning laser ophthalmoscope-based microperimetry. Optom Vis Sci. 2012; 89:563–574. [PubMed: 22446720]

Vaegan, Graham SL, Goldberg I, Buckland L, Hollows FC. Flash and pattern electroretinogram changes with optic atrophy and glaucoma. Exp Eye Res. 1995; 60:697–706. [PubMed: 7641852]

van der Schoot J, Vermeer KA, de Boer JF, Lemij HG. The effect of glaucoma on the optical attenuation coefficient of the retinal nerve fiber layer in spectral domain optical coherence tomography images. Invest Ophthalmol Vis Sci. 2012; 53:2424–2430. [PubMed: 22427540]

Vilupuru AS, Rangaswamy NV, Frishman LJ, Smith EL 3rd, Harwerth RS, Roorda A. Adaptive optics scanning laser ophthalmoscopy for in vivo imaging of lamina cribrosa. J Opt Soc Am A Opt Image Sci Vis. 2007; 24:1417–1425. [PubMed: 17429488]

Vohnsen B. Directional sensitivity of the retina: A layered scattering model of outer-segment photoreceptor pigments. Biomed Opt Express. 2014; 5:1569–1587. [PubMed: 24877016]

Wang B, Nevins JE, Nadler Z, Wollstein G, Ishikawa H, Bilonick RA, Kagemann L, Sigal IA, Grulkowski I, Liu JJ, Kraus M, Lu CD, Hornegger J, Fujimoto JG, Schuman JS. In vivo lamina cribrosa micro-architecture in healthy and glaucomatous eyes as assessed by optical coherence tomography. Invest Ophthalmol Vis Sci. 2013; 54:8270–8274. [PubMed: 24302585]

Wang L, Dong J, Cull G, Fortune B, Cioffi GA. Varicosities of intraretinal ganglion cell axons in human and nonhuman primates. Invest Ophthalmol Vis Sci. 2003a; 44:2–9. [PubMed: 12506048]

Wang Q, Kocaoglu OP, Cense B, Bruestle J, Jonnal RS, Gao W, Miller DT. Imaging retinal capillaries using ultrahigh-resolution optical coherence tomography and adaptive optics. Invest Ophthalmol Vis Sci. 2011a; 52:6292–6299. [PubMed: 21245397]

Wang Q, Tuten WS, Lujan BJ, Holland J, Bernstein PS, Schwartz SD, Duncan JL, Roorda A. Adaptive optics microperimetry and OCT images show preserved function and recovery of cone visibility in macular telangiectasia type 2 retinal lesions. Invest Ophthalmol Vis Sci. 2015; 56:778–786. [PubMed: 25587056]

Wang X, Li S, Fu J, Wu G, Mu D, Li S, Wang J, Wang N. Comparative study of retinal nerve fibre layer measurement by RTVue OCT and GDx VCC. Br J Ophthalmol. 2011b; 95:509–513. [PubMed: 20657017]

Wang Y, Zhao K, Jin Y, Niu Y, Zuo T. Changes of higher order aberration with various pupil sizes in the myopic eye. J Refract Surg. 2003b; 19:S270–274. [PubMed: 12699188]

Weinreb RN, Aung T, Medeiros FA. The pathophysiology and treatment of glaucoma: a review. JAMA. 2014; 311:1901–1911. [PubMed: 24825645]

Weinreb RN, Khaw PT. Primary open-angle glaucoma. Lancet. 2004; 363:1711–1720. [PubMed: 15158634]

Williams D, Yoon GY, Porter J, Guirao A, Hofer H, Cox I. Visual benefit of correcting higher order aberrations of the eye. J Refract Surg. 2000; 16:S554–559. [PubMed: 11019871]

Williams DR. Imaging single cells in the living retina. Vision Res. 2011; 51:1379–1396. [PubMed: 21596053]

Wolfing JI, Chung M, Carroll J, Roorda A, Williams DR. High-resolution retinal imaging of cone-rod dystrophy. Ophthalmology. 2006; 113:1019, e1011. [PubMed: 16650474]

Author Manuscript Author Manuscript Author Manuscript Author Manuscript

Wollstein G, Schuman JS, Price LL, Aydin A, Stark PC, Hertzmark E, Lai E, Ishikawa H, Mattox C, Fujimoto JG, Paunescu LA. Optical coherence tomography longitudinal evaluation of retinal nerve fiber layer thickness in glaucoma. Arch Ophthalmol. 2005; 123:464–470. [PubMed: 15824218]

Wu H, de Boer JF, Chen TC. Diagnostic capability of spectral-domain optical coherence tomography for glaucoma. Am J Ophthalmol. 2012; 153:815–826. e812. [PubMed: 22265147]

Wygnanski T, Desatnik H, Quigley HA, Glovinsky Y. Comparison of ganglion cell loss and cone loss in experimental glaucoma. Am J Ophthalmol. 1995; 120:184–189. [PubMed: 7639302]

Yang Z, Tatham AJ, Zangwill LM, Weinreb RN, Zhang C, Medeiros FA. Diagnostic ability of retinal nerve fiber layer imaging by swept-source optical coherence tomography in glaucoma. Am J Ophthalmol. 2015; 159:193–201. [PubMed: 25448991]

Zawadzki RJ, Capps AG, Kim DY, Panorgias A, Stevenson SB, Hamann B, Werner JS. Progress on Developing Adaptive Optics-Optical Coherence Tomography for Retinal Imaging: Monitoring and Correction of Eye Motion Artifacts. IEEE J Sel Top Quantum Electron. 2014; 20

Zawadzki RJ, Cense B, Zhang Y, Choi SS, Miller DT, Werner JS. Ultrahigh-resolution optical coherence tomography with monochromatic and chromatic aberration correction. Opt Express. 2008; 16:8126–8143. [PubMed: 18545525]

Zawadzki RJ, Choi SS, Fuller AR, Evans JW, Hamann B, Werner JS. Cellular resolution volumetric in vivo retinal imaging with adaptive optics-optical coherence tomography. Opt Express. 2009; 17:4084–4094. [PubMed: 19259248]

Zawadzki RJ, Choi SS, Jones SM, Oliver SS, Werner JS. Adaptive optics-optical coherence tomography: optimizing visualization of microscopic retinal structures in three dimensions. J Opt Soc Am A Opt Image Sci Vis. 2007; 24:1373–1383. [PubMed: 17429483]

Zawadzki RJ, Jones SM, Olivier SS, Zhao M, Bower BA, Izatt JA, Choi S, Laut S, Werner JS. Adaptive-optics optical coherence tomography for high-resolution and high-speed 3D retinal in vivo imaging. Opt Express. 2005; 13:8532–8546. [PubMed: 19096728]

Zhang X, Hu J, Knighton RW, Huang XR, Puliafito CA, Jiao S. Dual-band spectral-domain optical coherence tomography for in vivo imaging the spectral contrasts of the retinal nerve fiber layer. Opt Express. 2011; 19:19653–19659. [PubMed: 21996906]

Zhang Y, Cense B, Rha J, Jonnal RS, Gao W, Zawadzki RJ, Werner JS, Jones S, Olivier S, Miller DT. High-speed volumetric imaging of cone photoreceptors with adaptive optics spectral-domain optical coherence tomography. Opt Express. 2006; 14:4380–4394. [PubMed: 19096730]

Zhang Y, Rha J, Jonnal R, Miller D. Adaptive optics parallel spectral domain optical coherence tomography for imaging the living retina. Opt Express. 2005; 13:4792–4811. [PubMed: 19495398]

Zhong Z, Song H, Chui TY, Petrig BL, Burns SA. Noninvasive measurements and analysis of blood velocity profiles in human retinal vessels. Invest Ophthalmol Vis Sci. 2011; 52:4151–4157. [PubMed: 21467177]

Author Manuscript Author Manuscript Author Manuscript Author Manuscript

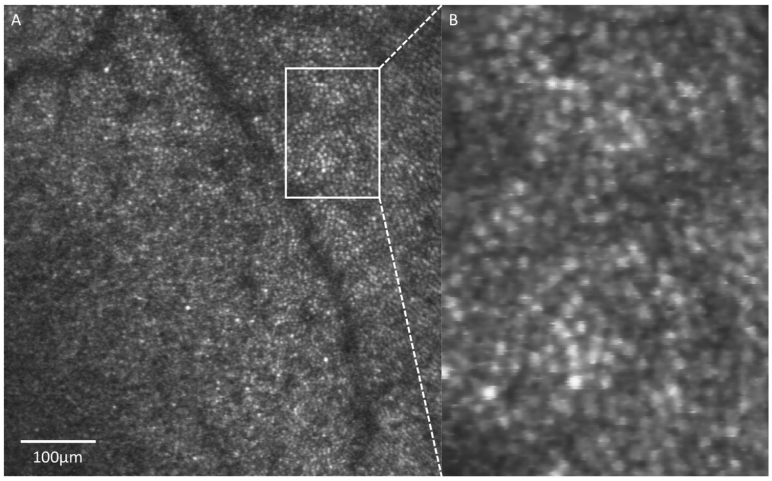

Figure 1.

AO-SLO of a healthy retina focused at the level of the photoreceptors in a 27-year-old Caucasian man. (B) Zoomed in region shows the ability to identify individual photoreceptors. Scale bar = 100 μm.

Author Manuscript Author Manuscript Author Manuscript Author Manuscript

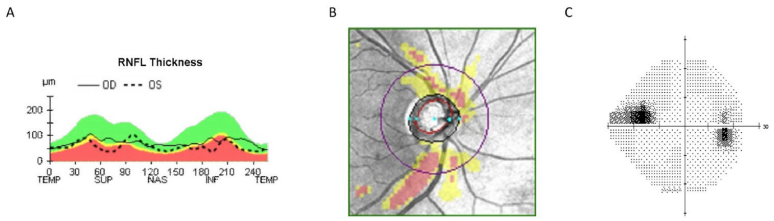

Figure 2.

Cirrus HD-OCT demonstrating inferior RNFL thinning in a 42-year-old Caucasian man with normal tension glaucoma (A, B) with corresponding superior nasal step scotoma (C).

Author Manuscript Author Manuscript Author Manuscript Author Manuscript

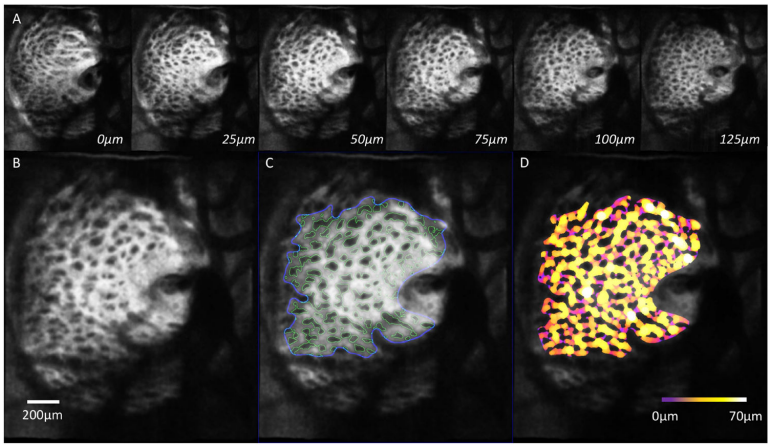

Figure 3.

(A) En-face slices from LC scan taken from the same subject with normal tension glaucoma shown in Figure 2, going from anterior to posterior in 25 μm increments. (B) Zoomed in C-mode slice from the same subject with (C) automated segmentation of corresponding slice with pores outlined in green and the boundary of segmentation area in blue. (D) 3D thickness analysis show regions of thick LC beams (white/yellow) and thin LC beams (purple). Scale bar = 200 μm.

Author Manuscript Author Manuscript Author Manuscript Author Manuscript

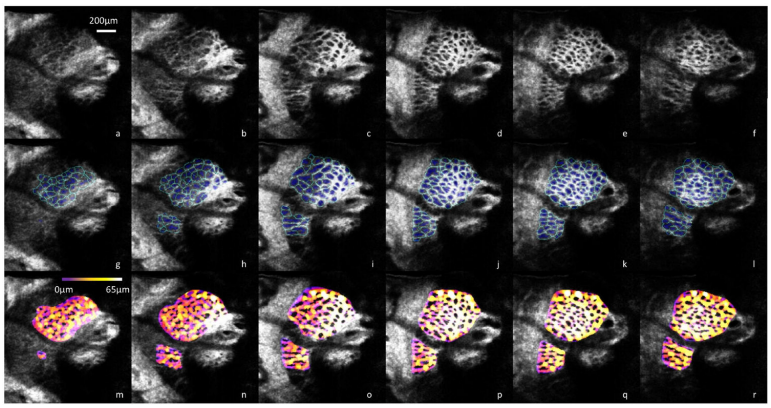

Figure 4.

AO-SD-OCT scan of a LC taken from a healthy 25-year-old Asian man (a–f) going anterior to posterior in 25 μm increments. Automated segmentation of pores in blue and beams in teal (g–l) allow further quantitative analysis such as beam thickness (m–r), with thicker beams in white/yellow and thinner beams in purple. Scale bar = 200 μm.

Author Manuscript Author Manuscript Author Manuscript Author Manuscript

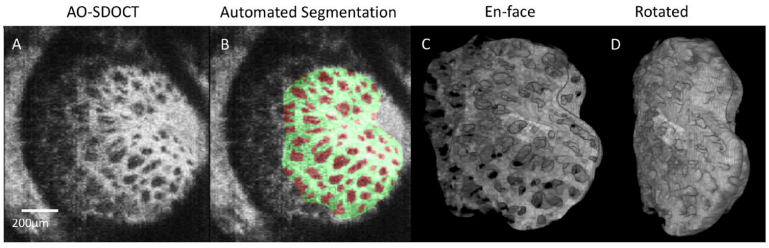

Figure 5.

(A) Original C-mode of adaptive optics OCT taken from a 56-year-old Caucasian woman with glaucoma. (B) Automated segmentation of the corresponding slice, with the beams labeled in green and pores in red. (C) 3D view en-face of the LC beams. (D) rotated 3D view of the same LC beams.

Author Manuscript Author Manuscript Author Manuscript Author Manuscript

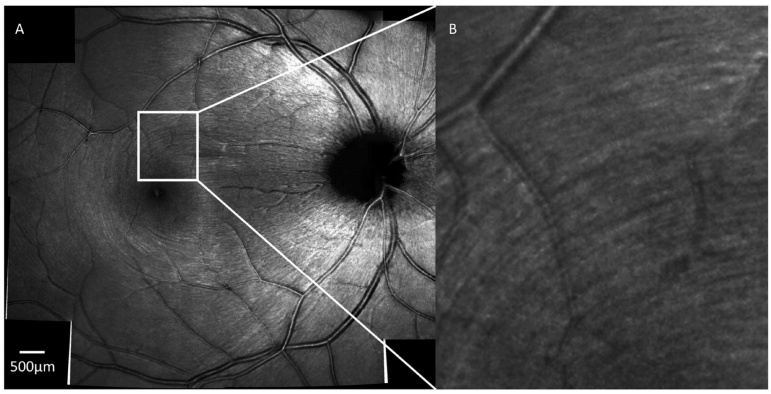

Figure 6.

(A) Montage AO-SLO scan of a healthy 27-year-old Caucasian man with the focus at the level of the RNFL with a zoomed in region (B) showing the striation of RNFL fiber bundles. Scale bar = 500 µm.